

The Straight-Line RAC Drawing Problem is NP-Hard

*Evmorfia N. Argyriou*¹ *Michael A. Bekos*² *Antonios Symvonis*¹

¹School of Applied Mathematics & Physical Sciences,
National Technical University of Athens, Greece

²Institute for Informatic,
University of Tübingen, Germany

Abstract

A *RAC drawing* of a graph is a polyline drawing in which every pair of crossing edges intersects at right angle. In this paper, we focus on straight-line RAC drawings and demonstrate an infinite class of graphs with unique RAC combinatorial embedding. We employ members of this class in order to show that it is \mathcal{NP} -hard to decide whether a graph admits a straight-line RAC drawing.

Submitted: October 2011	Reviewed: March 2012	Revised: April 2012	Accepted: August 2012	Final: August 2012
Published: September 2012				
Article type: Regular paper		Communicated by: S.-H. Hong		

The work of E.N. Argyriou has been co-financed by the European Union (European Social Fund - ESF) and Greek national funds through the Operational Program “Education and Lifelong Learning” of the National Strategic Reference Framework (NSRF) - Research Funding Program: Heracleitus II. Investing in knowledge society through the European Social Fund. The work of M.A. Bekos is implemented within the framework of the Action “Supporting Postdoctoral Researchers” of the Operational Program “Education and Lifelong Learning” (Action’s Beneficiary: General Secretariat for Research and Technology), and is co-financed by the European Social Fund (ESF) and the Greek State.

E-mail addresses: fargyriou@math.ntua.gr (Evmorfia N. Argyriou) bekos@informatik.uni-tuebingen.gr (Michael A. Bekos) symvonis@math.ntua.gr (Antonios Symvonis)

1 Introduction

In the graph drawing literature, the problem of finding aesthetically pleasant drawings of graphs has been extensively studied. The graph drawing community has introduced and studied several criteria that judge the quality of a graph drawing, such as the number of crossings among pairs of edges, the number of edge bends, the maximum edge length, the total area occupied by the drawing and so on (see [5, 18]).

Motivated by the fact that edge crossings have negative impact on the human understanding of a graph drawing [21, 22, 24], a great amount of research effort has been devoted on the problem of finding drawings with minimum number of edge crossings. Ideally, a graph would be desirable to be drawn without edge crossings. Graphs that admit such drawings are called *planar* graphs. Unfortunately, not all graphs are planar. It is known that any planar graph with n vertices has at most $3n - 6$ edges. Therefore, dealing with edge crossings is quite common when drawing graphs. Besides, the edge crossing minimization problem is \mathcal{NP} -complete in general [12]. Fortunately, recent eye-tracking experiments by Huang et al. [16, 17] indicate that the negative impact of an edge crossing is eliminated in the case where the crossing angle is greater than 70 degrees. These results motivated the study of a new class of drawings, called *right-angle drawings* or *RAC drawings* for short [1, 6, 7, 8]. A RAC drawing of a graph is a polyline drawing in which every pair of crossing edges intersects at right angle.

Didimo, Eades and Liotta [7] proved that it is always feasible to construct a RAC drawing of a given graph with at most three bends per edge. In this paper, we prove that the problem of determining whether an input graph admits a straight-line RAC drawing is \mathcal{NP} -hard. To do so, we first demonstrate a class of graphs with unique RAC combinatorial embedding (i.e., the cyclic order of edges incident to each vertex).

1.1 Related Work

Didimo, Eades and Liotta [7] initiated the study of RAC drawings and showed that any straight-line RAC drawing with n vertices has at most $4n - 10$ edges. They also demonstrated a class of n -vertices graphs with exactly $4n - 10$ edges and proved that any graph admits a RAC drawing with at most three bends per edge. Eades and Liotta [10] showed that every RAC graph with n vertices and $4n - 10$ edges (such graphs are called *maximally dense*) is 1-planar, i.e, it admits a drawing in which every edge is crossed by at most one other edge. A slightly weaker bound on the number of edges of an n -vertices RAC drawing was given by Arikushi et al. [3], who proved that any straight-line RAC drawing with n vertices may have $4n - 8$ edges. Angelini et al. [1] showed that the problem of determining whether an acyclic planar digraph admits a straight-line upward RAC drawing is \mathcal{NP} -hard. Furthermore, they constructed digraphs admitting straight-line upward RAC drawings that require exponential area. Di Giacomo et al. [6] studied the interplay between the crossing resolution, the maximum

number of bends per edges and the required area. Didimo et al. [8] presented a characterization of complete bipartite graphs that admit a straight-line RAC drawing. Arikushi et al. [3] studied polyline RAC drawings in which each edge has at most one or two bends and proved that the number of edges is at most $O(n)$ and $O(n \log^2 n)$, respectively. Dujmovic et al. [9] studied α -*Angle Crossing* (or αAC for short) drawings, i.e., drawings in which the smallest angle formed by an edge crossing is at least α . In their work, they presented upper and lower bounds on the number of edges. Van Kreveld [23] studied how much better (in terms of required area, edge-length and angular resolution) a RAC drawing of a planar graph can be than any planar drawing of the same graph.

Closely related to the RAC drawing problem, is the angular resolution maximization problem, i.e., the problem of maximizing the smallest angle formed by any two adjacent edges incident to a common vertex. Note that both problems correlate the resolution of a graph with the visual distinctiveness of the edges in a graph drawing. Formann et al. [11] introduced the notion of the angular resolution of straight-line drawings. In their work, they proved that determining whether a graph of maximum degree d admits a drawing of angular resolution $\frac{2\pi}{d}$ (i.e., the obvious upper bound) is \mathcal{NP} -hard. They also presented upper and lower bounds on the angular resolution for several types of graphs of maximum degree d . Malitz and Papakostas [20] proved that for any planar graph of maximum degree d , it is possible to construct a planar straight-line drawing with angular resolution $\Omega(\frac{1}{7d})$. Garg and Tamassia [14] presented a continuous trade-off between the area and the angular resolution of planar straight-line drawings. For the case of connected planar graphs with n vertices and maximum degree d , Gutwenger and Mutzel [15] presented a linear time algorithm that constructs planar polyline grid drawings on a $(2n - 5) \times (\frac{3}{2}n - \frac{7}{2})$ grid with at most $5n - 15$ bends and minimum angle greater than $\frac{2}{d}$. Bodlaender and Tel [4] showed that planar graphs with angular resolution at least $\frac{\pi}{2}$ are rectilinear. Lin and Yen [19] presented a force-directed algorithm based on edge-edge repulsion that constructs drawings with high angular resolution. Argyriou et al. [2] studied a generalization of the crossing and angular resolution maximization problems, in which the minimum of these quantities is maximized and presented optimal algorithms for complete and complete bipartite graphs and a force-directed algorithm for general graphs.

The rest of this paper is structured as follows: In Section 2, we introduce preliminary properties and notation. In Section 3, we present a class of RAC graphs with unique RAC combinatorial embedding. In Section 4, we show that the straight-line RAC drawing problem is \mathcal{NP} -hard. We conclude in Section 5 with open problems.

2 Preliminaries

Let $G = (V, E)$ be a simple, undirected graph drawn in the plane. We denote by $\Gamma(G)$ the drawing of G . Each drawing uniquely defines cyclic orders of edges incident to the same vertex and, therefore, specifies a combinatorial embedding.

Given a drawing $\Gamma(G)$ of a graph G , we denote by $\ell_{u,v}$ the line passing through vertices u and v . By $\ell'_{u,v}$, we refer to the semi-line that emanates from vertex u , towards vertex v . Similarly, we denote by $\ell_{u,v,w}$ ($\ell'_{u,v,w}$) the line (semi-line) that passes through (emanates from) vertex u and is perpendicular to edge (v, w) . Let (u, v) and (u, v') be a pair of non-overlapping edges incident to the same vertex. We say that (u, v) and (u, v') form a *fan anchored* at u . The following properties are used in the rest of this paper.

Property 1 (Didimo, Eades and Liotta [7]) *In a straight-line RAC drawing there do not exist three mutually crossing edges.*

Property 2 (Angelini et al. [1]) *In a straight-line RAC drawing no edge can cross a fan.*

Property 3 (Didimo, Eades and Liotta [7]) *In a straight-line RAC drawing there does not exist a triangle \mathcal{T} formed by edges of the graph and two edges (a, b) and (a, b') , such that a lies outside \mathcal{T} and b, b' lie inside \mathcal{T} .*

3 A Class of Graphs with Unique RAC Combinatorial Embedding

The main result of this paper, i.e., the \mathcal{NP} -hardness of the straight line RAC drawing problem, employs a reduction from the well-known 3-SAT problem [13]. However, before we proceed with the reduction details, we first provide a graph, referred to as *augmented square antiprism graph* (or *ASA graph* for short), which has the following property: “*The straight-line RAC drawings of the ASA graph define exactly two combinatorial embeddings*”. Fig. 1 shows the ASA graph and its two combinatorial embeddings (the fact that these are the only two RAC combinatorial embeddings will be proved later in this section). Observe that the ASA graph consists of a “central” vertex v_0 , which is incident to all vertices of the graph, and two quadrilaterals (refer to the dashed and bold drawn squares in Fig. 1a), that are denoted by \mathcal{Q}_1 and \mathcal{Q}_2 in the remainder of this paper. Removing the central vertex, the remaining graph corresponds to the skeleton of a square antiprism, and, it is commonly referred to as *square antiprism graph*.

If, in the ASA graph, we replace the two quadrilaterals with two triangles, then the resulting graph is the *augmented triangular antiprism graph*. Didimo, Eades and Liotta [7], who showed that any n -vertex graph which admits a RAC-drawing can have at most $4n - 10$ edges, used the augmented triangular antiprism graph, as an example of a graph that achieves the bound of $4n - 10$ edges (see Fig. 1.c in [7]). In contrast to the augmented triangular antiprism graph, the augmented square antiprism graph does not achieve this upper bound. In general, the class of *the augmented k -gon antiprism graphs*, $k \geq 3$, is a class of non-planar graphs, that all admit RAC drawings. Recall that any planar n -vertex graph has at most $3n - 6$ edges, and since an augmented k -gon antiprism

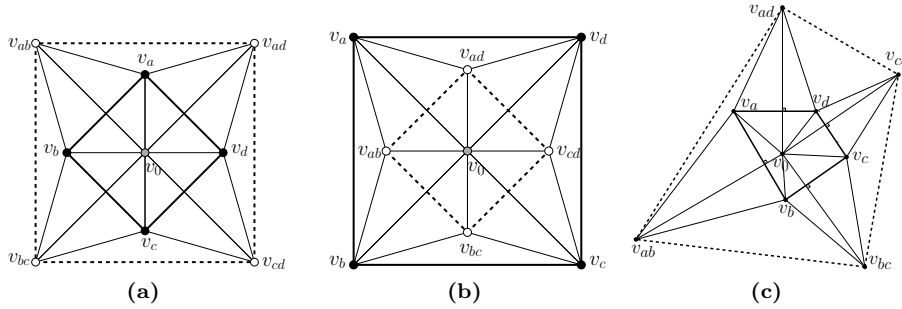


Figure 1: (a),(b) Two different RAC drawings of the ASA graph with different combinatorial embeddings. (a),(c) Two different RAC drawings of the ASA graph with the same combinatorial embedding.

graph has $2k + 1$ vertices and $6k$ edges, it is not planar for the entire class of these graphs.

Lemma 1 *There does not exist a RAC drawing of the ASA graph in which i) the central vertex v_0 lies on the exterior of quadrilateral Q_i and ii) an edge connecting v_0 to a vertex of Q_i crosses another edge of Q_i , $i = 1, 2$.*

Proof: Let Q be one of quadrilaterals Q_i , $i = 1, 2$ and let v_a, v_b, v_c and v_d be its vertices, consecutive along quadrilateral Q (refer to Fig. 2). Assume, to the contrary, that vertex v_0 lies on the exterior of quadrilateral Q and there exists an edge, say (v_0, v_a) , that emanates from vertex v_0 towards vertex v_a of quadrilateral Q , such that it crosses an edge, say (v_b, v_c) ¹, of Q (see Fig. 2). On the ASA graph, vertices v_b and v_c have the following properties: (a) they are both connected to vertex v_0 , and, (b) they have a common neighbor v_{bc} , which is incident to vertex v_0 and $v_{bc} \notin Q$ (see Fig. 1).

Observe that if vertex v_{bc} lies in the non-shaded regions of Fig. 2, then at least one of the edges incident to v_{bc} crosses either (v_0, v_a) or (v_b, v_c) , which are already involved in a right-angle crossing. This leads to a situation where three edges mutually cross, which, by Property 1 is not permitted. Hence, vertex v_{bc} should lie in the interior of the gray-shaded regions R_1, R_2 or R_3 in Fig. 2. In the following, we consider each of these cases separately. Note that, depending on the position of v_a, v_b, v_c , and, v_0, R_2 or R_3 or $R_2 \cup R_3$ may be empty.

Case i: *Vertex v_{bc} lies in the interior of R_1 .* This case is depicted in Fig. 3. Let $T_{v_{bc}}$ be the region formed by vertices v_{bc}, v_b and v_c (i.e., the dark-gray shaded region of Fig. 3). Vertex v_d , which has to be connected to vertices v_a and v_c , and, the central vertex v_0 , cannot lie within $T_{v_{bc}}$, since (v_a, v_0) and (v_a, v_d) form a fan anchored at v_a and crossed by (v_b, v_c) , which by Property 2 is not permitted. Since vertex v_d has to be connected to vertex v_0 , it has to lie either on semi-line $\ell'_{v_0, v_c, v_{bc}}$ or on semi-line $\ell'_{v_0, v_b, v_{bc}}$. We consider only the former case.

¹The case where it crosses edge (v_c, v_d) is symmetric.

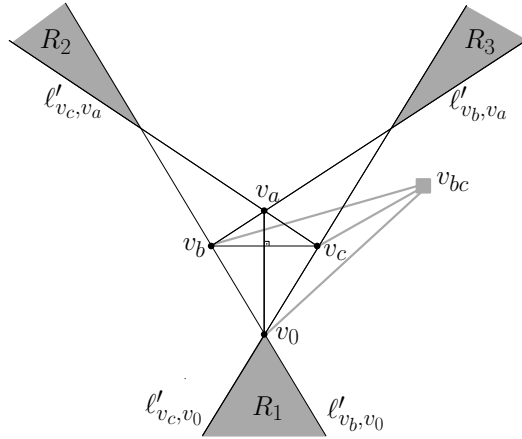


Figure 2: Configuration used in proof of Lemma 1: Vertex v_{bc} should lie in the interior of one of the regions R_1 , R_2 and R_3 .

The latter one is handled symmetrically. However, under this restriction, the common neighbor v_{cd} of vertices v_c and v_d cannot be connected to vertex v_0 , since edge (v_0, v_{cd}) should be perpendicular to one of the edges of $T_{v_{bc}}$. To see this, observe that if edge (v_0, v_{cd}) is perpendicular to (v_c, v_{bc}) , then (v_0, v_{cd}) and (v_0, v_d) form a fan anchored at v_0 and crossed by (v_c, v_{bc}) , which by Property 2 is not permitted (see Fig. 3a). Consider now the case where edge (v_0, v_{cd}) is perpendicular to edge (v_b, v_{bc}) (and lies on $l'_{v_0, v_b, v_{bc}}$; see Fig. 3b). Since angle $\widehat{v_c v_b v_{bc}}$ is acute, edge (v_b, v_{bc}) should be crossed by both edges (v_0, v_{cd}) and (v_c, v_{cd}) , which form a fan anchored at v_{cd} . This leads to a contradiction due to Property 2.

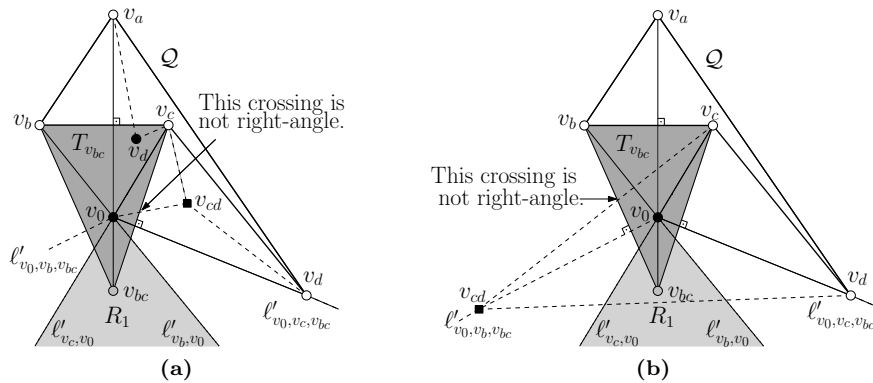


Figure 3: Configurations used in proof of Lemma 1: Vertex v_{bc} lies in the interior of R_1 .

Case ii: Vertex v_{bc} lies in the interior of either R_2 or R_3 . Assume, without loss

of generality, that vertex v_{bc} lies in the interior of R_3 . This case is depicted in Fig. 4. Let u be a vertex of the ASA graph (distinct from v_a, v_b, v_c and v_0) and assume that u lies in the interior of the triangle $T_{v_{bc}}$ formed by vertices v_b, v_c and v_{bc} . Vertex u has to be connected to the central vertex v_0 . Edge (v_0, u) should not be involved in crossings with neither edge (v_b, v_c) , since (v_0, u) and (v_0, v_a) would form a fan anchored at v_0 and crossed by (v_b, v_c) , nor edge (v_c, v_{bc}) , since angle $\widehat{v_b v_c v_{bc}}$ is smaller than 180° . Therefore, triangle $T_{v_{bc}}$ cannot accommodate any other vertex (except v_a). Now observe that each vertex of quadrilateral \mathcal{Q} has degree five and there do not exist three vertices of quadrilateral \mathcal{Q} , that have a common neighbor (see Fig. 1). These properties trivially hold for vertex v_a , since $v_a \in \mathcal{Q}$. Based on the above properties, each neighbor of vertex v_a can lie either in the interior of the dark-gray region of Fig. 4, or, on the external face of the already constructed drawing (along the dashed semi-lines $\ell'_{v_a, v_c, v_{bc}}$ and $\ell'_{v_a, v_b, v_{bc}}$ of Fig. 4, respectively). This implies that we can place only four vertices out of those incident to vertex v_a , i.e., one of them should lie in the interior of $T_{v_{bc}}$ and thus, it cannot be connected to vertex v_0 .

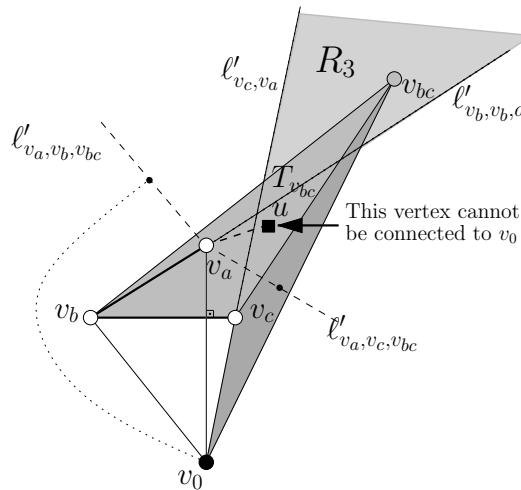


Figure 4: Configuration used in proof of Lemma 1: Vertex v_{bc} lies in the interior of R_3 .

From the above case analysis, it follows that the central vertex v_0 cannot lie on the exterior of quadrilateral \mathcal{Q} , so that an edge connecting v_0 to a vertex of \mathcal{Q} crosses another edge of \mathcal{Q} . \square

Lemma 2 *In any RAC drawing of the ASA graph, quadrilateral \mathcal{Q}_i is drawn planar, for each $i = 1, 2$.*

Proof: Let \mathcal{Q} be one of quadrilaterals \mathcal{Q}_i , $i = 1, 2$, and let, as in the proof of the previous lemma, v_a, v_b, v_c and v_d be its vertices, consecutive along quadrilateral \mathcal{Q} . Note that it is not feasible a non-planar, straight-line RAC drawing of

a quadrilateral to contain more than one right-angle crossing (the drawing of \mathcal{Q} forms two orthogonal triangles). Assume to the contrary that in a RAC drawing of the ASA graph, quadrilateral \mathcal{Q} is not drawn planar, and say that edges (v_a, v_b) and (v_c, v_d) form a right-angle crossing. This case is illustrated in Fig. 5a. In the following, we will consider the cases where the central vertex v_0 lies either in one of the orthogonal triangles or in the area outside them. In both cases, we will reach a contradiction.

Case i: *Vertex v_0 lies in the interior of one of the two triangles.* Assume without loss of generality that vertex v_0 (which is incident to all vertices of quadrilateral \mathcal{Q}) lies in the interior of the triangle formed by vertices v_b, v_c and the intersection point, say w , of edges (v_a, v_b) and (v_c, v_d) , as in Fig. 5a. In this case, edges (v_a, v_0) and (v_a, v_b) form a fan anchored at v_a , which is crossed by (v_c, v_d) . This is not possible due to Property 2.

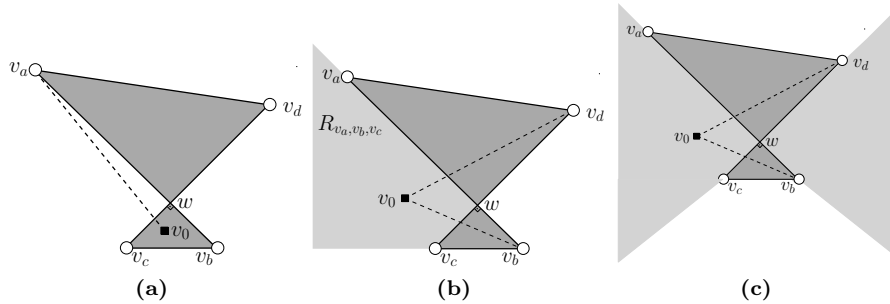


Figure 5: Configurations used in proof of Lemma 2: Quadrilateral \mathcal{Q} is not drawn planar. (a) v_0 cannot lie within one of the two triangles, (b) v_0 cannot lie within R_{v_a, v_b, v_c} , and, (c) v_0 cannot lie within the light-gray open areas.

Case ii: *Vertex v_0 lies outside the two triangles.* Without loss of generality, we assume that edge (v_b, v_c) is horizontal and that edge (v_a, v_d) is drawn above it. See Fig. 5a. The two triangles are drawn dark-shaded.

Let R_{v_a, v_b, v_c} denote the light-gray shaded open area defined by angle $\widehat{v_a v_b v_c}$ which excludes the area of triangle $\triangle w v_b v_c$. See Fig. 5b. We first show that vertex v_0 cannot lie in area R_{v_a, v_b, v_c} . To see that, simply observe that if v_0 lied within area R_{v_a, v_b, v_c} , then edges (v_0, v_b) and (v_0, v_d) would form a fan anchored at v_0 and crossed by (v_c, v_d) , which is not possible due to Property 2. In the same way, we can define the open areas R_{v_b, v_c, v_d} , R_{v_c, v_d, v_a} and R_{v_d, v_a, v_b} and show that vertex v_0 cannot lie in any of them. Thus, it remains to examine the case where vertex v_0 lies either in the white area below edge (v_b, v_c) or in the white area above edge (v_a, v_d) . See Fig. 5c. We only consider the former case since the later can be similarly handled by assuming that (v_a, v_d) is the horizontal edge.

So, assume that vertex v_0 lies in the white area of Fig. 5c below edge (v_b, v_c) .

Given this assumption, we can state the following propositions regarding the placement of the remaining vertices in a RAC drawing of the ASA graph.

Proposition 1 *Edge (v_b, v_c) should be inside triangle $\Delta v_a v_0 v_d$.*

Proof: Refer to Fig. 6a. For the sake of contradiction assume that edge (v_b, v_c) is not inside triangle $\Delta v_a v_0 v_d$. Then, one of the triangle’s edges incident at v_0 would cross a fan formed by edges of \mathcal{Q} anchored either at v_b or v_c , which is a contradiction due to Property 2. \square

Proposition 2 *Vertex v_{bc} lies inside triangle $\Delta v_a v_0 v_d$.*

Proof: Refer to Fig. 6b. Vertex v_{bc} is connected to both v_b and v_c , which by Proposition 1 are inside triangle $\Delta v_a v_0 v_d$. By Property 3, it follows that vertex v_{bc} must also lie inside triangle $\Delta v_a v_0 v_d$. \square

Proposition 3 *Vertex v_{ab} lies inside triangle $\Delta v_0 v_c x$, where x is the intersection point of line ℓ_{v_b, v_c} with edge (v_0, v_a) .*

Proof: Refer to Fig. 6c. In order to prove this proposition, we will prove that vertex v_{ab} (a) cannot lie outside triangle $\Delta v_a v_0 v_d$, (b) must lie below line ℓ_{v_b, v_c} , and, cannot lie in either (d) triangle $\Delta v_0 v_b y$, or, (e) triangle $\Delta v_0 v_b v_c$.

- (a) *Vertex v_{ab} lies inside triangle $\Delta v_a v_0 v_d$:* Vertex v_{ab} is connected to v_b and v_{bc} , which by Propositions 1 and 2, respectively, lie within $\Delta v_a v_0 v_d$. This ensures that v_{ab} lies inside triangle $\Delta v_a v_0 v_d$, as well; otherwise Property 3 is violated.
- (b) *Vertex v_{ab} must lie below line ℓ_{v_b, v_c} :* Let y be the intersection point of line ℓ_{v_b, v_c} with edge (v_0, v_d) . For the sake of contradiction assume that v_{ab} lies above line ℓ_{v_b, v_c} . We consider the following cases. First assume that v_{ab} lies within quadrilateral $v_a x v_c v_d$. Then, edges (v_a, v_b) and (v_b, v_{ab}) form a fan anchored at v_b which is crossed by (v_c, v_d) . In the case where v_{ab} lies within triangle $\Delta v_c y v_d$ then edges (v_a, v_b) and (v_a, v_{ab}) form a fan anchored at v_a which is crossed by (v_c, v_d) . Since both cases lead to a contradiction Property 2, we conclude that v_{ab} must lie below line ℓ_{v_b, v_c} .
- (c) *Vertex v_{ab} cannot lie in triangle $\Delta v_0 v_b y$:* This is due to the fact that v_{ab} is connected with v_a . If edge (v_{ab}, v_a) passes from the “left” of v_b it must enter and exit triangle $\Delta v_0 v_b v_c$, forming three mutually crossing edges. If edge (v_{ab}, v_a) passes from the “right” of v_b , then (v_a, v_{ab}) and (v_a, v_b) form a fan anchored at v_a and crossed by (v_c, v_d) . Since both cases lead to a contradiction (due to Properties 1 and 2, respectively), we conclude that v_{ab} cannot lie in triangle $\Delta v_0 v_b y$.
- (d) *Vertex v_{ab} cannot lie in triangle $\Delta v_0 v_b v_c$:* This is, again, due to the fact that v_{ab} is connected with v_a . If edge (v_a, v_{ab}) passes from the “right” of v_c , then it must enter and exit triangle $\Delta v_b v_c w$, forming three mutually crossing edges. However, this is not permitted due

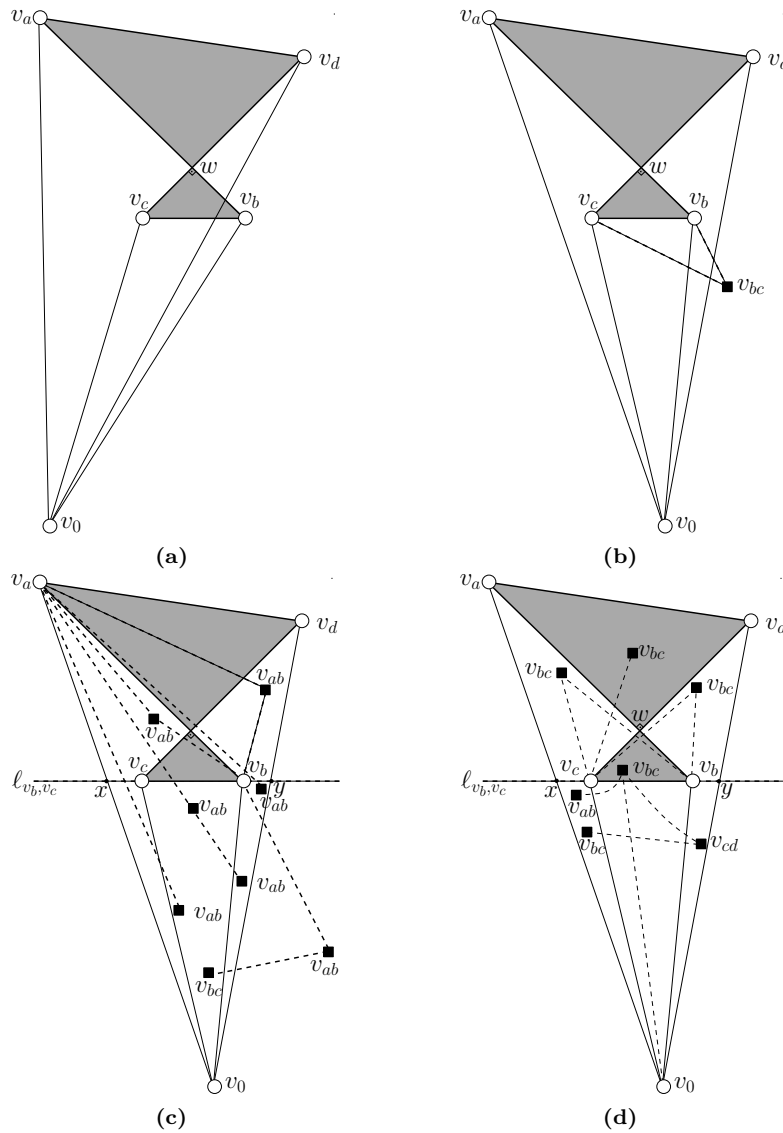


Figure 6: Configurations used in proof of Lemma 2 (Propositions 1-5): (a) Edge (v_b, v_c) does not lie inside triangle $\triangle v_a v_0 v_d$. (b) Vertex v_{bc} does not lie inside triangle $\triangle v_a v_0 v_d$, (c) Potential placements of vertex v_{ab} , (d) Potential placements of vertex v_{bc}

to Property 1. If edge (v_a, v_{ab}) passes from the “left” of v_c , then it must cross at right angle edge (v_c, v_0) . But, since edge (v_a, v_b) is also perpendicular to edge (v_c, v_d) then quadrilateral $v_a v_d v_c v_0$ must be

convex, and thus, v_0 must be above line ℓ_{v_b, v_c} , a clear contradiction.

□

Proposition 4 *Vertex v_{cd} lies inside triangle $\Delta v_0 v_b y$.*

Proof: Following symmetric arguments as in the proof of Proposition 3.

□

Proposition 5 *Vertex v_{bc} lies within triangle $\Delta v_0 y v_c$.*

Proof: Recall that by Proposition 2 v_{bc} lies within triangle $\Delta v_0 v_a v_d$. In order to establish that vertex v_{bc} lies within triangle $\Delta v_0 y v_c$, we will lead to a contradiction the cases where vertex v_{bc} lies within quadrilaterals (a) $v_a w v_c x$ and (b) $v_d w v_b y$, and within triangles (c) $\Delta v_a w v_d$, (d) $\Delta v_b w v_c$ and (e) $\Delta x v_c v_0$. Refer to Fig. 6d.

- (a) *Vertex v_{bc} does not lie within quadrilateral $v_a w v_c x$:* If it does, then edges (v_a, v_b) and (v_b, v_{bc}) form a fan anchored at v_b which is crossed by (v_c, v_d) .
- (b) *Vertex v_{bc} does not lie within quadrilateral $v_d w v_b y$:* If it does, then edges (v_c, v_d) and (v_c, v_{bc}) form a fan anchored at v_c which is crossed by (v_a, v_b) .
- (c) *Vertex v_{bc} does not lie within triangle $\Delta v_a w v_d$:* If it does, then edges (v_c, v_d) and (v_c, v_{bc}) form a fan anchored at v_c which is crossed by (v_a, v_b) .
- (d) *Vertex v_{bc} does not lie within triangle $\Delta v_b w v_c$:* If it does, then it has three neighbors, namely v_0, v_{ab} and v_{cd} , outside triangle $\Delta v_b w v_c$. Thus, it must be connected to them by edges that exit different sides of the triangle. Given that v_0 lies below line ℓ_{v_b, v_c} , then at least one of v_{ab} and v_{cd} must be above line ℓ_{v_b, v_c} . A clear contradiction.
- (e) *Vertex v_{bc} does not lie within triangle $\Delta x v_c v_0$:* Recall that by Proposition 4 vertex v_{cd} lies inside triangle $\Delta v_0 v_b y$. However, vertex v_{bc} is connected to vertex v_{cd} . This implies that if vertex v_{bc} lies within triangle $\Delta x v_c v_0$, then (v_{bc}, v_{cd}) must enter and exit triangle $\Delta v_0 v_b v_c$, forming three mutually crossing edges.

□

Since vertex v_{ab} lies inside triangle $\Delta v_0 v_c x$ (Proposition 3), and, vertex v_{bc} lies within triangle $\Delta v_0 y v_c$ (Proposition 5), edges (v_{ab}, v_{bc}) and (v_{ab}, v_b) form a fan anchored at v_{ab} which is crossed by (v_0, v_c) . This is impossible due to Property 2. Thus, by assuming a legal RAC drawing of the ASA graph where vertex v_0 is outside the two triangles, we concluded that it is not possible to find a legal placement for v_{bc} ; a clear contradiction. This completes the proof of Case ii of this lemma.

□

Lemma 3 *In any RAC drawing of the ASA graph, the central vertex v_0 lies in the interior of quadrilateral \mathcal{Q}_i , $i = 1, 2$.*

Proof:

From Lemma 2, it follows that quadrilateral \mathcal{Q}_i should be drawn planar, for each $i = 1, 2$. In order to prove this lemma, we assume to the contrary that central vertex v_0 lies on the exterior of one of the two quadrilaterals, say w.l.o.g., on the exterior of quadrilateral \mathcal{Q}_1 . Let v_a, v_b, v_c and v_d be \mathcal{Q}_1 's vertices, consecutive along quadrilateral \mathcal{Q}_1 . Then, by Lemma 1, vertex v_0 cannot contribute additional crossings on quadrilateral \mathcal{Q}_1 . This suggests that the drawing of the graph induced by quadrilateral \mathcal{Q}_1 and vertex v_0 will be planar and resemble the ones depicted in Fig. 7. We denote by $T_{\mathcal{Q}_1}$ the triangle formed by vertex v_0 and the two vertices, which are on the convex hull of $\mathcal{Q}_1 \cup v_0$ (refer to the gray-shaded triangles of Fig. 7).

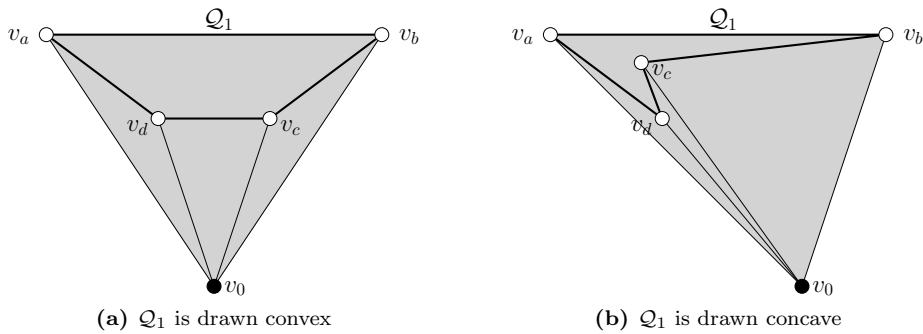


Figure 7: Configurations used in proof of Lemma 3: Different drawings of the graph induced by quadrilateral \mathcal{Q}_1 and vertex v_0 .

Proposition 6 *No vertex of \mathcal{Q}_2 lies outside $T_{\mathcal{Q}_1}$.*

Proof: Refer to Fig. 7 and assume w.l.o.g that $T_{\mathcal{Q}_1}$ is defined by vertices v_0, v_a and v_b , i.e., v_a and v_b are on the convex hull of $\mathcal{Q}_1 \cup v_0$. In the following, we prove that each of the vertices of \mathcal{Q}_2 should lie inside $T_{\mathcal{Q}_1}$.

- (a) *Vertex v_{cd} lies within triangle $T_{\mathcal{Q}_1}$:* If not, Property 3 is violated (see Fig. 8a); v_{cd} is connected to v_c and v_d , which both lie inside $T_{\mathcal{Q}_1}$.
- (b) *Vertex v_{bc} lies within triangle $T_{\mathcal{Q}_1}$:* If not, Property 3 is violated (see Fig. 8b); v_{bc} is connected to v_c and v_{cd} , which both lie inside $T_{\mathcal{Q}_1}$.
- (c) *Vertex v_{ad} lies within triangle $T_{\mathcal{Q}_1}$:* If not, Property 3 is violated (see Fig. 8c); v_{ad} is connected to v_d and v_{cd} , which both lie inside $T_{\mathcal{Q}_1}$.
- (d) *Vertex v_{ab} lies within triangle $T_{\mathcal{Q}_1}$:* If not, Property 3 is violated (see Fig. 8d); v_{ab} is connected to v_{ad} and v_{bc} , which both lie inside $T_{\mathcal{Q}_1}$.

□

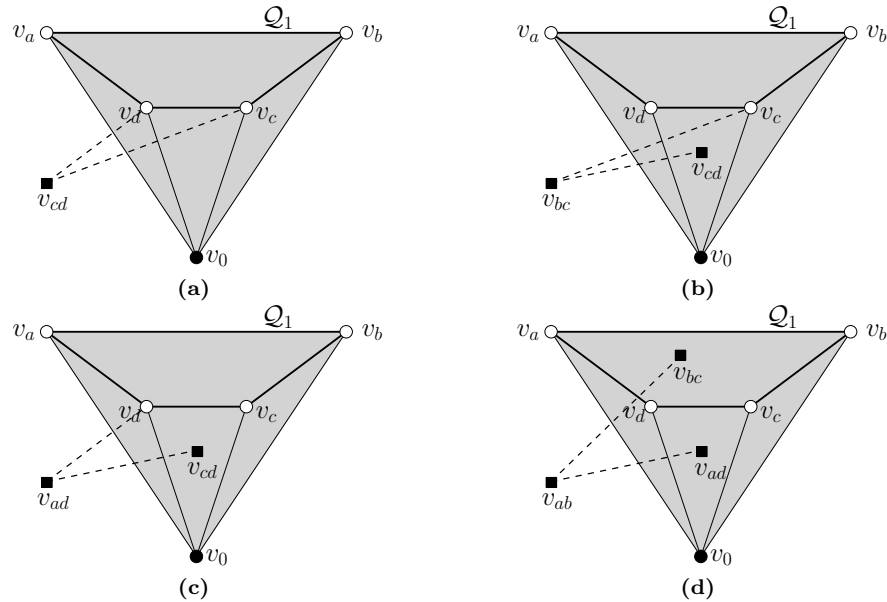


Figure 8: Configurations used in proof of Lemma 3 (Proposition 6): All vertices of \mathcal{Q}_2 should lie inside $T_{\mathcal{Q}_1}$

Since \mathcal{Q}_2 lies inside $T_{\mathcal{Q}_1}$, vertex v_0 is external to \mathcal{Q}_2 as well. Therefore, in a way similar to that of Proposition 6, one can also prove that \mathcal{Q}_1 lies inside $T_{\mathcal{Q}_2}$, where $T_{\mathcal{Q}_2}$ is defined by vertex v_0 and the two vertices, which are on the convex hull of $\mathcal{Q}_2 \cup v_0$. However, this leads to a contradiction, since two triangles (i.e., $T_{\mathcal{Q}_1}$ and $T_{\mathcal{Q}_2}$) cannot be nested to each other without being identical, and thus introducing vertex and edge overlaps. \square

Lemma 4 *In any RAC drawing of the ASA graph, all edges from the central vertex v_0 to quadrilateral \mathcal{Q}_i are fully contained into \mathcal{Q}_i , $i = 1, 2$.*

Proof: By Lemma 3, vertex v_0 should lie in the interior of quadrilateral \mathcal{Q}_i , $i = 1, 2$, which is drawn planar due to Lemma 2. If both \mathcal{Q}_1 and \mathcal{Q}_2 are drawn convex, then the lemma trivially holds. For the sake of contradiction, assume that \mathcal{Q}_1 is drawn concave and an edge emanating from vertex v_0 towards a vertex of quadrilateral \mathcal{Q}_1 , say v_a , crosses an edge, say (v_c, v_d) , of quadrilateral \mathcal{Q}_1 (see Fig. 9).

Proposition 7 *The sum of the three acute internal angles of \mathcal{Q}_1 is less than $\frac{\pi}{2}$*

Proof: Since \mathcal{Q}_1 is concave at v_d , the internal angle at v_d is greater than $3\pi/2$. Hence the sum of the remaining internal angles is less than $\pi/2$. \square

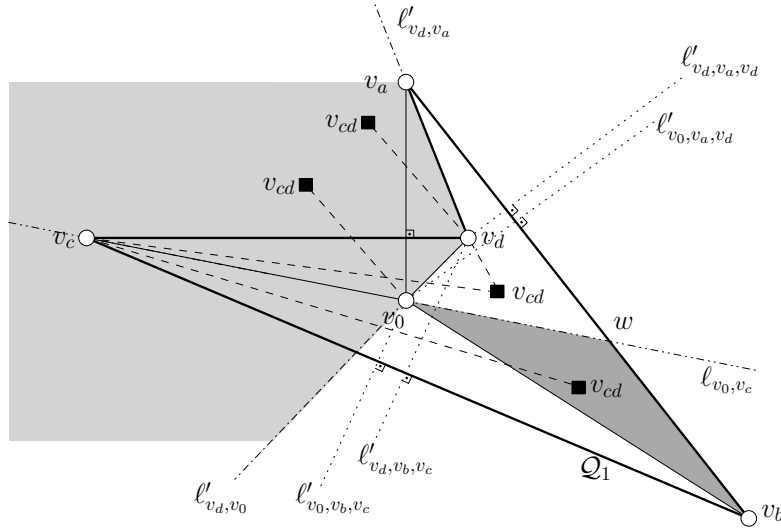


Figure 9: Configuration used in proof of Lemma 4 (Proposition 8): Potential placements of v_{cd} .

Proposition 8 *Vertex v_{cd} should lie in the interior of Q_1 .*

Proof: Recall that v_{cd} is connected to v_c , v_d and v_0 and assume, to the contrary, that vertex v_{cd} is not in the interior of Q_1 . Then, the following hold (refer to Fig. 9):

- i) *Edge (v_0, v_{cd}) is not entering Q_1 from (v_c, v_d) :* If it did, edges (v_0, v_{cd}) and (v_0, v_a) form a fan anchored at v_0 and crossed by (v_c, v_d) , which is not permitted due to Property 2.
- ii) *Edge (v_0, v_{cd}) is not entering Q_1 from (v_a, v_d) :* If it did, then it is implied that it is possible to draw from v_0 perpendicular line segments (i.e., (v_0, v_a) and (v_0, v_{cd})) to two edges forming the concave angle of Q_1 . However, this is not possible, since v_0 is internal to Q_1 .
- iii) *Edge (v_0, v_{cd}) is entering Q_1 either from (v_a, v_b) or (v_b, v_c) :* Trivially follows from (i) and (ii).
- iv) *Vertex v_{cd} is not in region formed by l'_{v_d, v_a} and l'_{v_d, v_0} and contains v_c :* In Fig. 9, this region is shaded in light-gray. It follows from the fact that (v_d, v_{cd}) cannot cross (v_0, v_a) , since otherwise edges (v_d, v_{cd}) and (v_c, v_d) form a fan anchored at v_d and crossed by (v_0, v_a) , which is not permitted due to Property 2.
- v) *Edge (v_d, v_{cd}) is entering Q_1 either from (v_a, v_b) or (v_b, v_c) :* Trivially follows from (iv).

From (iii) and (v), it follows that v_{cd} should be at the intersection of two semi-lines (refer to the dotted semi-lines of Fig. 9) which are perpendicular

to (v_a, v_b) and/or (v_b, v_c) . However, this is a contradiction since these lines do not intersect due to Proposition 7; they are perpendicular on two consecutive edges of \mathcal{Q}_1 that form an acute angle. \square

Proposition 9 *Vertex v_{cd} lies in the interior of $\triangle v_0v_bv_c$.*

Proof: By Proposition 8, it is enough to prove that v_{cd} lies “below” ℓ_{v_0,v_c} and not in $\triangle v_0v_bw$ (refer to the dark-gray shaded triangle of Fig. 9), where w is the intersection point of ℓ_{v_0,v_c} and (v_a, v_b) . The former property is obvious, since v_{cd} is connected to both v_c and v_d . Hence, if v_{cd} was “above” ℓ_{v_0,v_c} , then (v_c, v_d) and either (v_c, v_{cd}) or (v_d, v_{cd}) would form a fan anchored at either v_c or v_d , respectively, that is crossed by (v_0, v_a) . If v_{cd} is in the interior of $\triangle v_0v_bw$, then (v_c, v_{cd}) should cross (v_0, v_b) at right angle. However, this is not possible since the perpendicular line from v_c to (v_0, v_b) is external to $\triangle v_0v_bw$ due to Proposition 7. Hence, v_{cd} is in the interior of $\triangle v_0v_bv_c$ (and along ℓ'_{v_d,v_0,v_b} ; see Fig. 10), as desired. \square

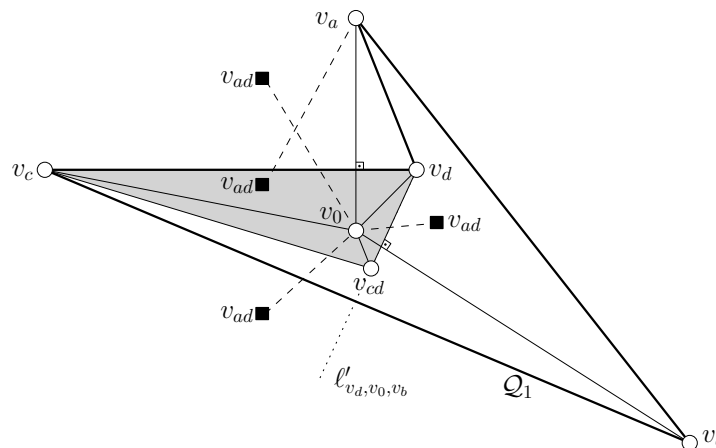


Figure 10: Configuration used in proof of Lemma 4 (Propositions 10-12): Potential placements of v_{ad} .

Proposition 10 *Vertex v_{ad} lies outside $\triangle v_cv_dv_{cd}$.*

Proof: In Fig. 10, triangle $\triangle v_cv_dv_{cd}$ is shaded in gray. Assume, to the contrary, that v_{ad} lies in the interior of $\triangle v_cv_dv_{cd}$. Then, since v_0 is internal as well, vertex v_a , which is outside $\triangle v_cv_dv_{cd}$, should be connected to v_0 and v_{ad} , that both lie in the interior of $\triangle v_cv_dv_{cd}$. This is a contradiction due to Property 3. \square

Proposition 11 *Edge (v_0, v_{ad}) cannot enter triangle $\triangle v_cv_dv_{cd}$ neither from (v_c, v_d) nor from (v_d, v_{cd}) .*

Proof: Follows from the fact that edges (v_c, v_d) and (v_d, v_{cd}) are already crossed at right angle by edges (v_0, v_a) and (v_0, v_b) , respectively, which are incident to v_0 , as is edge (v_0, v_{ad}) . \square

Proposition 12 *Vertex v_{ad} lies in the interior of $\Delta v_0 v_b v_c$.*

Proof: By Proposition 11, edge (v_0, v_{ad}) enters triangle $\Delta v_c v_d v_{cd}$ from (v_c, v_{cd}) . If v_{ad} was external to $\Delta v_0 v_b v_c$, edges (v_c, v_{cd}) and (v_b, v_c) should form a fan anchored at v_c and crossed by (v_0, v_{ad}) , which is not permitted due to Property 2. \square

Propositions 9 and 12 suggest that both v_{cd} and v_{ad} lie in the interior of $\Delta v_0 v_b v_c$. Based on this and following a similar reasoning scheme as in the proof of Proposition 6, we can prove that all vertices of \mathcal{Q}_2 should lie in the interior of $\Delta v_0 v_b v_c$. However, this is a contradiction since vertex v_0 should lie in the interior of \mathcal{Q}_2 , due to Lemma 3. \square

Lemma 5 *There does not exist a RAC drawing of the ASA graph, in which quadrilaterals \mathcal{Q}_1 and \mathcal{Q}_2 intersect.*

Proof: For the sake of contradiction, assume that \mathcal{Q}_1 and \mathcal{Q}_2 intersect. With slight abuse of notation, let v_a^i, v_b^i, v_c^i and v_d^i be \mathcal{Q}_i 's vertices consecutive along quadrilateral $\mathcal{Q}_i, i = 1, 2$, i.e., $\{v_a, v_b, v_c, v_d\} = \{v_a^1, v_b^1, v_c^1, v_d^1\}$ and $\{v_{ab}, v_{bc}, v_{cd}, v_{ad}\} = \{v_a^2, v_b^2, v_c^2, v_d^2\}$. Let w.l.o.g., $(v_a^1, v_b^1) \in \mathcal{Q}_1$ and $(v_a^2, v_b^2) \in \mathcal{Q}_2$ be a pair of vertices that are involved in the crossing of \mathcal{Q}_1 and \mathcal{Q}_2 and let w be their intersection point. Consider a RAC drawing of the ASA graph in which (v_a^2, v_b^2) is drawn horizontal (and, hence, (v_a^1, v_b^1) is drawn vertical) and assume that v_b^2 is to the left of v_a^2 , whereas v_b^1 is above v_a^1 (see Fig. 11).

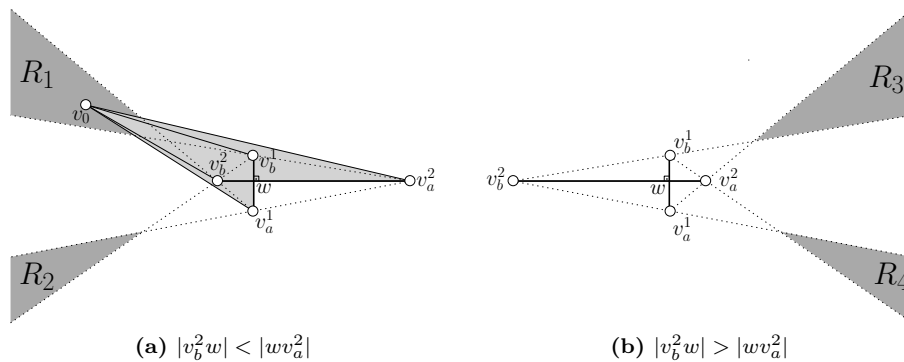


Figure 11: Configurations used in proof of Lemma 5: Vertex v_0 should lie in the interior of one of the regions R_1, R_2, R_3 and R_4 .

Edges (v_0, v_a^1) and (v_0, v_b^1) should not cross (v_a^2, v_b^2) since that would form a fan anchored at v_a^1 and v_b^1 , respectively, crossed by (v_a^2, v_b^2) , which is not

permitted due to Property 2. Similarly, edges (v_0, v_a^2) and (v_0, v_b^2) should not cross (v_a^1, v_b^1) . This suggests that vertex v_0 should lie in one of the dark-gray shaded unbounded regions of Fig. 11. Assume w.l.o.g that v_0 lies in R_1 (the remaining cases are treated symmetrically). Due to Lemma 3, v_0 is internal to \mathcal{Q}_1 . However, as we will show, there does not exist a legal placement of the vertices of \mathcal{Q}_2 , such that \mathcal{Q}_1 encloses v_0 . In the following, we first prove that v_c^1 should lie outside the light-gray shaded quadrilateral of Fig. 11a.

Proposition 13 *Vertex v_c^1 lies outside quadrilateral $wv_a^1v_0v_a^2$, where w is the intersection of $(v_a^1, v_b^1) \in \mathcal{Q}_1$ and $(v_a^2, v_b^2) \in \mathcal{Q}_2$.*

Proof: Refer to Fig. 12 and recall that quadrilateral \mathcal{Q}_1 is formed by vertices $v_a^1, v_b^1, v_c^1, v_d^1$ in this order. For the sake of contradiction, assume that v_c^1 lies inside quadrilateral $wv_a^1v_0v_a^2$. If v_d^1 lies inside quadrilateral $wv_a^1v_0v_a^2$ as well, then \mathcal{Q}_1 lies entirely within quadrilateral $wv_a^1v_0v_a^2$. Hence, v_0 is not in the interior of \mathcal{Q}_1 , which is a contradiction due to Lemma 3. Therefore, v_d^1 should be outside quadrilateral $wv_a^1v_0v_a^2$. Since v_c^1 is inside quadrilateral $wv_a^1v_0v_a^2$ and v_d^1 outside, edge (v_c^1, v_d^1) should be perpendicular to an edge of $wv_a^1v_0v_a^2$. This suggests that v_d^1 should lie within a dark-gray shaded region of Fig. 12, which implies again that v_0 is not in the interior of \mathcal{Q}_1 , since edge (v_d^1, v_a^1) forms a quadrilateral which does not enclose v_0 . A clear contradiction due to Lemma 3. □

Proposition 13 and Lemma 3 suggest that quadrilateral \mathcal{Q}_1 should be drawn as shown in Fig. 13, i.e., edge (v_b^1, v_c^1) should be perpendicular to (v_0, v_a^2) whereas vertex v_d^1 should be to the “left” of v_0 such that edges (v_c^1, v_d^1) and (v_a^1, v_d^1) do not cross quadrilateral $wv_a^1v_0v_a^2$ and v_0 is in the interior of \mathcal{Q}_1 . We proceed to investigate how \mathcal{Q}_2 is drawn.

Proposition 14 *Vertex v_c^2 lies outside quadrilateral $wv_a^1v_0v_a^2$, where w is the intersection of $(v_a^1, v_b^1) \in \mathcal{Q}_1$ and $(v_a^2, v_b^2) \in \mathcal{Q}_2$.*

Proof: Similarly to Proposition 13. □

Proposition 15 *Vertex v_c^2 lies in the interior \mathcal{Q}_1 .*

Proof: Proposition 14 implies that vertex v_c^2 lies outside quadrilateral $wv_a^1v_0v_a^2$. If in addition v_c^2 lies outside \mathcal{Q}_1 , then edges (v_0, v_a^1) and (v_d^1, v_a^1) form a fan at v_a^1 crossed by (v_b^2, v_c^2) , which is not permitted by Property 2 (see Fig. 13). □

From the above propositions it follows that vertex v_c^2 should lie outside quadrilateral $wv_a^1v_0v_a^2$ but in the interior of \mathcal{Q}_1 . In the following, we will prove that v_d^2 can neither lie in the interior of \mathcal{Q}_1 nor to its exterior, leading thus to a contradiction our initial hypothesis that \mathcal{Q}_1 and \mathcal{Q}_2 intersect. Refer to Fig. 13.

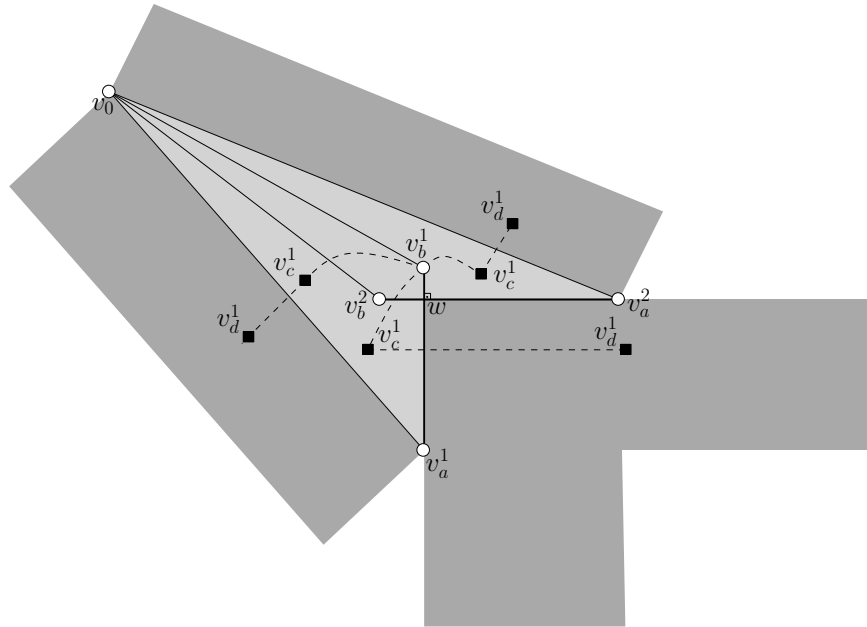


Figure 12: Configuration used in proof of Lemma 5 (Proposition 13): Potential placements of v_d^1 assuming that v_0 is in the interior of R_1 and v_c^1 in the interior of $wv_a^1v_0v_a^2$.

Proposition 16 *Vertex v_d^2 lies in the interior of \mathcal{Q}_1 .*

Proof: Assume to the contrary that v_d^2 lies outside \mathcal{Q}_1 . Then, it should reside within the dark-gray shaded unbounded region of Fig. 13, such that (v_c^2, v_d^2) is perpendicular to (v_a^1, v_d^1) . This implies that v_0 cannot lie in the interior of \mathcal{Q}_2 , since edge (v_d^2, v_a^2) forms a quadrilateral which does not enclose v_0 , which leads to a contradiction. Therefore, v_d^2 should lie in the interior of \mathcal{Q}_1 . \square

By Proposition 16, vertex (v_a^2, v_d^2) should perpendicularly cross an edge of \mathcal{Q}_1 , because v_d^2 is inside it whereas v_a^2 outside it. First observe that (v_a^2, v_d^2) can be perpendicular to neither (v_c^1, v_d^1) nor (v_a^1, v_d^1) . To see this assume, to the contrary, that (v_a^2, v_d^2) is perpendicular to (v_c^1, v_d^1) . Then, angle $\widehat{v_b^1 v_c^1 v_d^1}$ (denoted by ϕ in Fig. 13) should be greater than π , which contradicts the fact that v_0 is in the interior of \mathcal{Q}_1 . Similarly, we can prove that (v_a^2, v_d^2) cannot be perpendicular to (v_a^1, v_d^1) . Hence, (v_d^2, v_a^2) should be perpendicular to either (v_b^1, v_c^1) or (v_a^1, v_b^1) . In the case where (v_d^2, v_a^2) crosses (v_b^1, v_c^1) , edges (v_d^2, v_a^2) and (v_0, v_a^2) form a fan anchored at v and crossed by (v_b^1, v_c^1) , which by Property 2 is not permitted. Similarly, (v_d^2, v_a^2) cannot be perpendicular to (v_a^1, v_b^1) . Therefore, v_d^2 cannot lie in the interior of \mathcal{Q}_1 , contradicting Proposition 16. \square

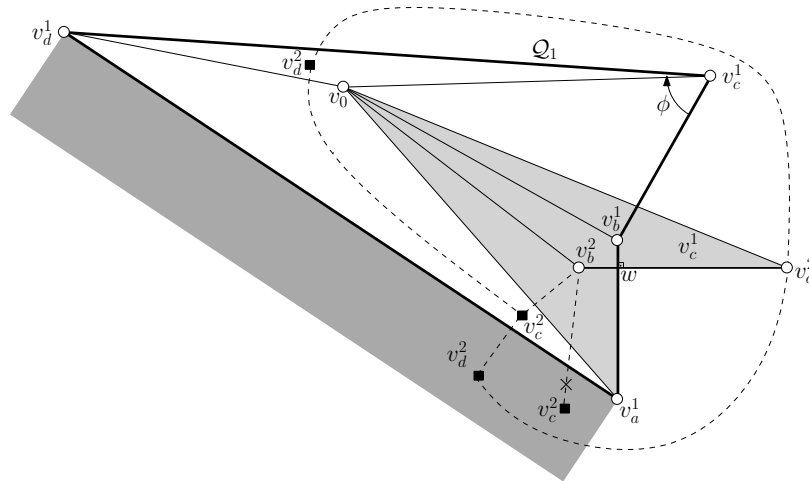


Figure 13: Configuration used in proof of Lemma 5: Potential placements of v_d^2 assuming that v_0 is in the interior of R_1 and v_c^2 lies outside $wv_a^1v_0v_a^2$ but in the interior of Q_1 .

Theorem 1 *The straight-line RAC drawings of the ASA graph define exactly two combinatorial embeddings.*

Proof: So far, we have managed to prove that both quadrilaterals Q_1 and Q_2 are drawn planar, do not cross, and have central vertex v_0 to their interiors. This suggests that either quadrilateral Q_1 is in the interior of Q_2 , or quadrilateral Q_2 is in the interior of Q_1 . However, in both cases vertex v_0 , which has to be connected to the four vertices of the “external” quadrilateral, should inevitably perpendicularly cross the four edges of the “internal” quadrilateral. This implies only two feasible combinatorial embeddings. The two combinatorial embeddings are shown in Fig. 1a and 1b. \square

We extend the ASA graph by appropriately *glueing* multiple instances of it, the one next to the other. Fig. 14a demonstrates how this operation is realized on two instances, say G and G' , of the ASA graph, i.e., by identifying two “external” vertices, say v and v' , of G with two “external” vertices of G' (refer to the gray-shaded vertices of Fig. 14a), and by employing an additional edge (refer to the dashed drawn edge of Fig. 14a), which connects an “internal” vertex, say u , of G with the corresponding “internal” vertex, say u' , of G' . Let $G \oplus G'$ be the graph produced by the glueing operation on G and G' . Since the RAC drawings of G and G' define two combinatorial embeddings each, one would expect that the RAC drawings of $G \oplus G'$ would define four possible combinatorial embeddings. We will show that this is not true and, more precisely, that there exists only a single combinatorial embedding.

Theorem 2 *Let G and G' be two instances of the ASA graph. Then, the*

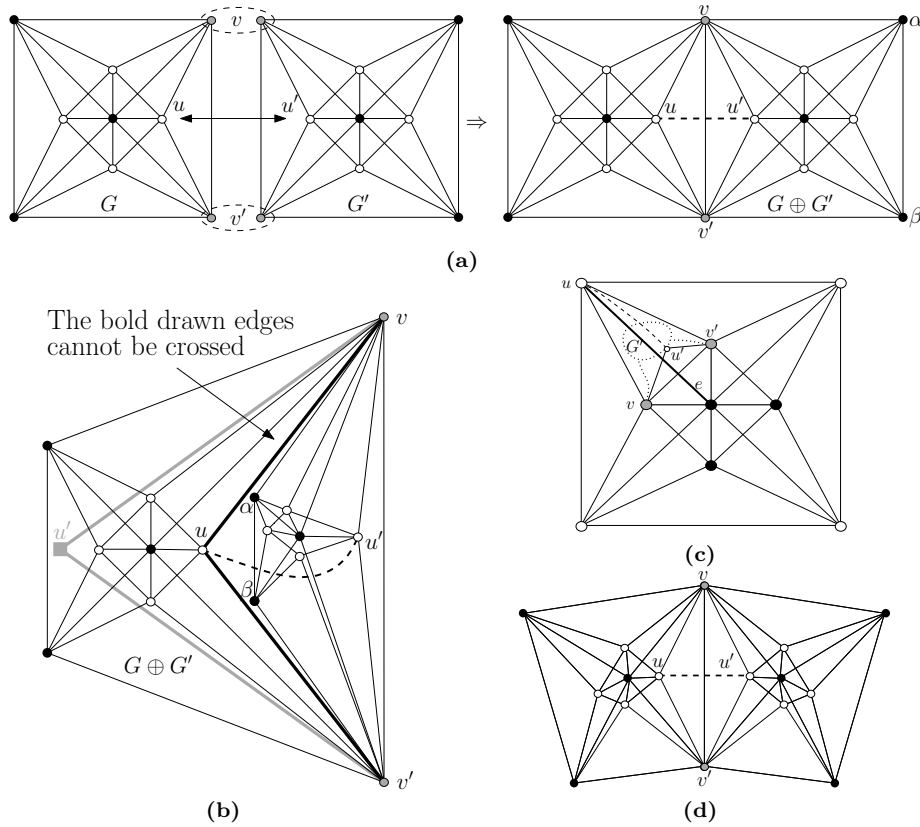


Figure 14: (a) Glueing two instances of the ASA graph, (b) The additional (dashed) edge does not permit the second instance to be drawn in the interior of the first one. (c) The vertices, which are identified during the glueing operation (v and v' in figure), should be on the external face of each ASA graph. (d) Each glueing operation may introduce a “turn” in the corresponding RAC drawing.

straight-line RAC drawings of $G \oplus G'$ define a single RAC combinatorial embedding.

Proof: Obviously, in any RAC drawing of $G \oplus G'$, both G and G' should be drawn RAC. Say that in a RAC drawing of $G \oplus G'$, G is drawn such that vertices v and v' (that are identified during the glueing operation) are on the external face of $\Gamma(G)$.² Then, the common neighbor of v and v' in G' that is not identified with v_0 (i.e., u') can be either in the interior of $\Gamma(G)$ or to its external face in the drawing of $G \oplus G'$.

We first consider the case where vertex u' is in the interior of $\Gamma(G)$ in the drawing of $G \oplus G'$ (see Fig. 14b). Vertex u' , which is incident to both v and

²The case where v and v' are not on the external face of $\Gamma(G)$ will be examined later.

v' , cannot reside to the “left” of both edges (u, v) and (u, v') (refer to the bold drawn edges of Fig. 14b), since this would lead to a situation where three edges mutually cross and, subsequently, to a violation of Property 1 (see the gray-shaded square vertex of Fig. 14b). Therefore, vertex u' should lie within the triangular face of G formed by vertices u, v and v' . Similarly, the same holds for the central vertex of G' , which is also incident to vertices v and v' . By Property 3, any common neighbor of vertices u' and v should also lie within the same triangular face of G , which progressively implies that the entire graph G' should reside within this face, as in Fig. 14b. Since vertices v and v' are on the external face of $\Gamma(G')$ in the drawing of $G \oplus G'$ and G' should be drawn RAC, vertices α and β in Fig. 14b should be on the external face of $\Gamma(G')$ as well (due to Theorem 1). However, in this case and since u' is incident to v and v' , edge (u, u') , which is employed during the glueing operation, crosses the interior of G' , which is not permitted. This suggests that if vertex u' is in the interior of $\Gamma(G)$ in the drawing of $G \oplus G'$, then there is no feasible embedding.

If one assumes that u' is on the external face of $\Gamma(G)$ in the drawing of $G \oplus G'$, then it can be similarly proved that the entire graph G' should be on this face, too. Hence, v and v' are on the external face of $\Gamma(G')$, as well. From the discussion above it follows that v and v' are on the external face of both $\Gamma(G)$ and $\Gamma(G')$ in the drawing of $G \oplus G'$, which implies a feasible embedding (see Fig. 14d).

We now examine the case where v and v' are not on the external face of $\Gamma(G)$ in a RAC drawing of $G \oplus G'$, i.e., v and v' are along the internal quadrilateral of G in the RAC drawing of $G \oplus G'$. This is illustrated in Fig. 14c. Let e be the edge of G , which perpendicularly crosses edge (v, v') and emanates from the external quadrilateral towards the central vertex of G (refer to the bold solid edge of Fig. 14c). Edge e will be involved in crossings with G' . Let u' be the common neighbor of v and v' in G' . Then, $e, (v, v')$ and either (v, u') or (u', v') form three mutually crossing edges in the drawing of $G \oplus G'$, which is not permitted due to Property 1.

Therefore, the vertices that are identified during a glueing operation should always be on the external face of each ASA graph and, subsequently, any drawing of $G \oplus G'$ has unique combinatorial embedding. \square

Note that the RAC drawing of $G \oplus G'$ may differ from the drawing of Fig. 14a. In the general case, each glueing operation may introduce a “turn” in the corresponding RAC drawing, as in Fig. 14d. However, the combinatorial embedding is still the same.

4 The Straight-Line RAC Drawing Problem is NP-hard

In this Section, we will reduce the well-known 3-SAT problem [13] to the straight-line RAC drawing problem. In a 3-SAT instance, we are given a formula ϕ in conjunctive normal form with variables x_1, x_2, \dots, x_n and clauses

C_1, C_2, \dots, C_m , each with three literals. We show how to construct a graph G_ϕ that admits a straight-line RAC drawing $\Gamma(G_\phi)$ if and only if formula ϕ is satisfiable. Fig. 17 shows an example of a graph which is build by our reduction based on a particular input 3-SAT formula. Our proof follows the general approach of Formann et al. [11] (used to prove that the angular resolution maximization problem is \mathcal{NP} -hard) using different gadgets to encode the variables and the clauses of the given formula.

4.1 Description of the Construction

Fig. 15 illustrates the gadgets of our construction. Each gray-shaded square in these drawings corresponds to an ASA graph. Adjacent gray squares correspond to glued ASA graphs (refer, for example, to the topmost gray squares of Fig. 15a). There also exist gray squares that are not adjacent, but connected through edges. The legend in Fig. 15 describes how these connections are realized.

The gadget that encodes variable x_i of formula ϕ is given in Fig. 15a. It consists of a combination of ASA graphs, and, “horizontal” and “vertical” edges, which form a tower, such that the RAC drawings of each tower define a single combinatorial embedding. One side of the tower accommodates multiple vertices that correspond to literal x_i , whereas its opposite side accommodates vertices that correspond to its negation \bar{x}_i (refer to vertices $x_{i,1}, \dots, x_{i,m}$ and $\bar{x}_{i,1}, \dots, \bar{x}_{i,m}$ in Fig. 15a). These vertices are called *variable endpoints*. Then, based on whether on the final drawing the negated vertices will appear to the “left” or to the “right” side of the tower, we will assign a true or a false value to variable x_i , respectively. Pairs of consecutive endpoints $x_{i,j}$ and $x_{i,j+1}$ are separated by a *corridor* (marked by a “tick” in Fig. 15a), which allows perpendicular edges to pass through it (see the bottommost dashed arrow of Fig. 15a). Note that no edge can pass through a “corridor” formed on a variable endpoint (marked by a cross in Fig. 15a), since there exist four non-parallel edges that “block” any other edge passing through them (see the topmost dashed arrow of Fig. 15a). The corridors can have variable height. In the variable gadget of variable x_i , there are also two vertices (drawn as gray circles in Fig. 15a), which have degree four. These vertices serve as “connectors” among consecutive variable gadgets, i.e., these vertices should be connected to their corresponding vertices on the variable gadgets of variables x_{i-1} and x_{i+1} . Note that the connector vertices of the variable gadgets associated with variables x_1 and x_n are connected to connectors of the variable gadgets that correspond to variables x_2 and x_{n-1} , respectively, and to connectors of *dummy variable gadgets*.

Fig. 15b illustrates a dummy variable gadget, which (similarly to the variable gadget) consists of a combination of ASA graphs, and, “horizontal” and “vertical” edges, which form a tower. The RAC drawings of this gadget also define a single combinatorial embedding. A dummy variable gadget does not support vertices that correspond to literals. However, it contains connector vertices (they are drawn as gray circles in Fig. 15b). In our construction, we use exactly two dummy variable gadgets. The connector vertices of each dummy

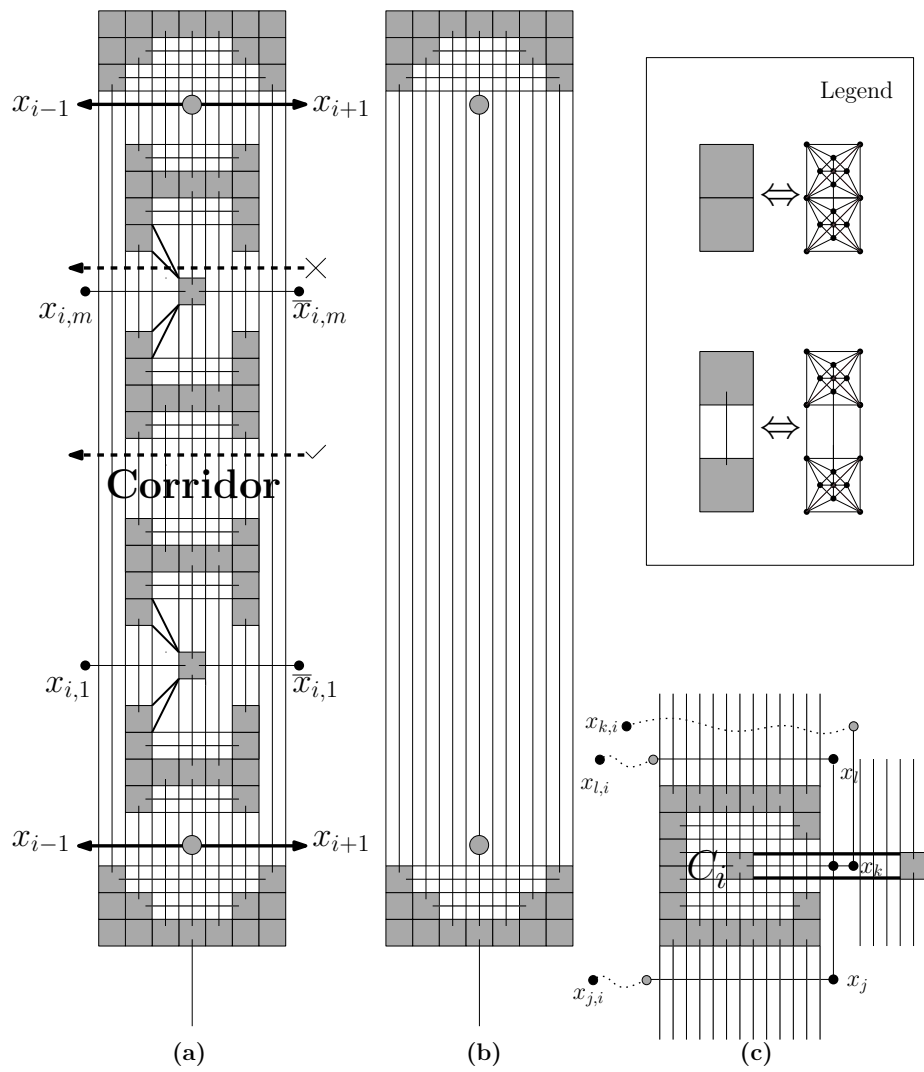


Figure 15: Gadgets of our construction: (a) Variable gadget, (b) Dummy variable gadget, (c) Clause gadget

variable gadget should be connected to their corresponding connector vertices on the variable gadgets associated with variables x_1 and x_n , respectively.

The gadget that encodes the clauses of formula ϕ is illustrated in Fig. 15c and resembles to a valve. Let $C_i = (x_j \vee x_k \vee x_l)$ be a clause of ϕ . As illustrated in Fig. 15c, the gadget which corresponds to clause C_i contains three vertices³, say x_j , x_k , and x_l , such that: x_j has to be connected to $x_{j,i}$, x_k to $x_{k,i}$ and x_l to $x_{l,i}$ by paths of length two. These vertices, referred to as the *clause endpoints*, encode the literals of each clause. Obviously, if a clause contains a negated literal, it should be connected to the negated endpoint of the corresponding variable gadget. The clause endpoints are incident to a vertex “trapped” within two parallel edges (refer to the bold drawn edges of Fig. 15c). Therefore, in a RAC drawing of G_ϕ , only two of them can perpendicularly cross these edges, one from top (*top endpoint*) and one from bottom (*bottom endpoint*). The other one (*right endpoint*) should remain in the interior of the two parallel edges. The one that will remain “trapped” on the final drawing will correspond to the true literal of this clause.

The gadgets, which correspond to variables and clauses of ϕ , are connected together by the skeleton of graph G_ϕ , which is depicted in Fig. 16a. The skeleton consists of two main parts, i.e., one “horizontal” and one “vertical”. The vertical part accommodates the clause gadgets (see Fig. 16a). The horizontal part will be used in order to “plug” the variable gadgets. The long edges that perpendicularly cross (refer to the crossing edges slightly above the horizontal part in Fig. 16a), imply that the vertical part should be perpendicular to the horizontal part. The horizontal part of the skeleton is separately illustrated in Fig. 16b. Observe that it contains one set of horizontal lines, which in conjunction with the vertical edges of the variable and clause gadgets do not allow it to bend.

Fig. 17 shows how the variable gadgets are attached to the skeleton. More precisely, this is accomplished by a single edge, which should perpendicularly cross the set of the horizontal edges of the horizontal part. Therefore, each variable gadget is perpendicularly attached to the skeleton, as in Fig. 17. Note that each variable gadget should be drawn completely above these horizontal edges, since otherwise the connections among variable endpoints and clause endpoints would not be feasible. The connector vertices of the dummy variable gadgets, the variable gadgets and the vertical part of the construction, ensure that the variable gadgets will be parallel to each other (i.e., they are not allowed to bend) and parallel to the vertical part of the construction.

4.2 Properties of the Construction

We now proceed to investigate some properties of our construction. Any path of length two that emanates from a top- or bottom-clause endpoint can reach a variable endpoint either on the left or on the right side of its associated variable

³With slight abuse of notation, the same term is used to denote variables of ϕ and vertices of G_ϕ .

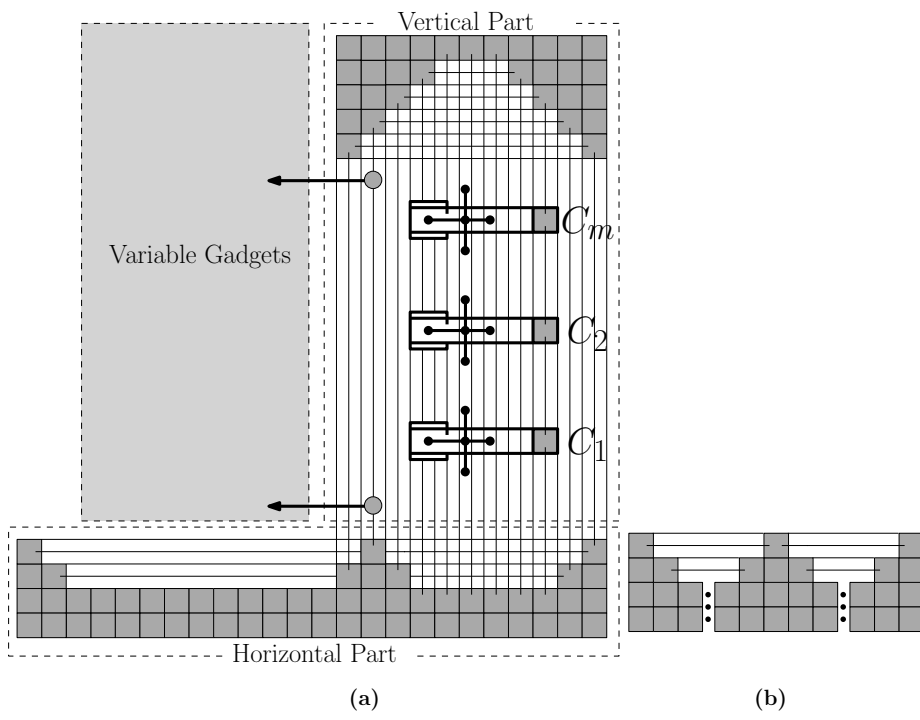


Figure 16: Illustration of the skeleton of the construction.

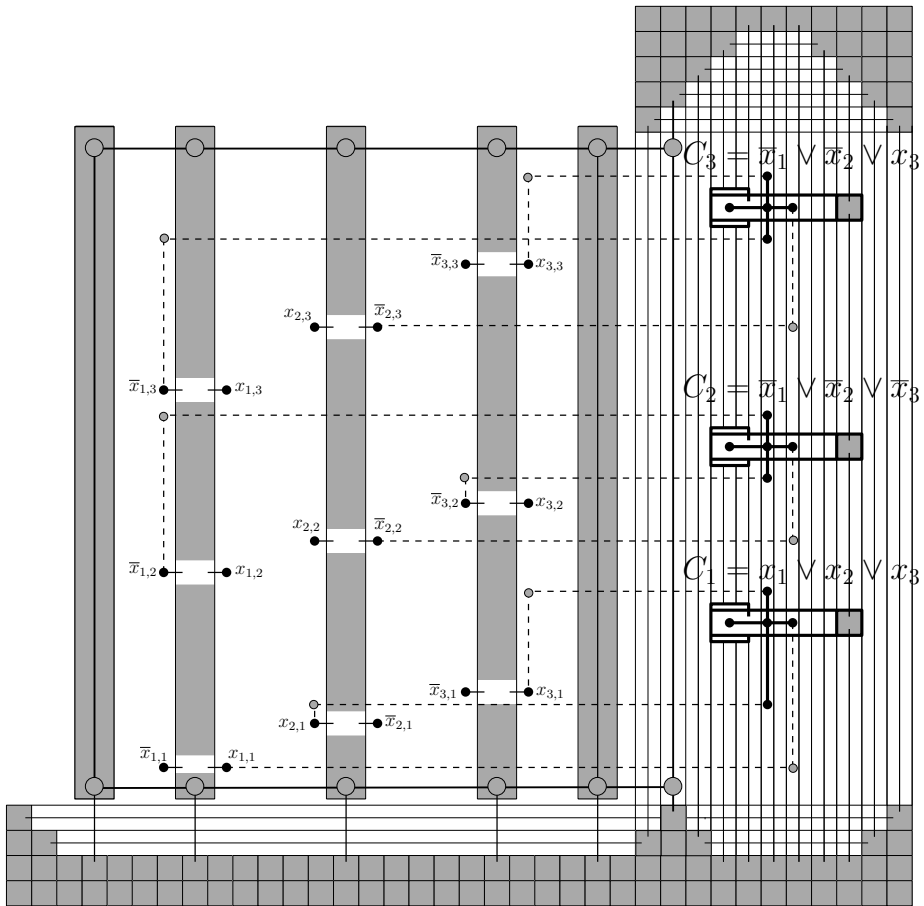


Figure 17: The reduction from 3-SAT to the straight-line RAC drawing problem. The input formula is $\phi = (x_1 \vee x_2 \vee x_3) \wedge (\bar{x}_1 \vee \bar{x}_2 \vee \bar{x}_3) \wedge (\bar{x}_1 \vee \bar{x}_2 \vee x_3)$. The drawing corresponds to the truth assignment $x_1 = x_3 = \text{true}, x_2 = \text{false}$.

gadget. The first edge of this path should perpendicularly cross the vertical edges of the vertical part of the construction and pass through some corridors⁴, whereas the second edge will be used to realize the “final” connection with the variable gadget endpoint (see Fig. 17).

The same doesn’t hold for the paths that emanate from a right-clause endpoint. These paths can only reach variable endpoints on the right side of their associated variable gadgets. More precisely, the first edge of the 2-length path should cross one of the two parallel edges (refer to the bold drawn edges of Fig. 15c) that “trap” it, whereas the other one should be used to reach (passing through variable corridors) its variable endpoint (see Fig. 17).

Our construction ensures that up to translations, rotations and stretchings any RAC drawing of G_ϕ looks like the one of Fig. 17.

4.3 Reduction from 3-SAT

Theorem 3 *It is \mathcal{NP} -hard to decide whether an input graph admits a straight-line RAC drawing.*

Proof: It is clear that the construction can be completed in $O(nm)$ time. Assume now that there is a RAC drawing $\Gamma(G_\phi)$ of G_ϕ . If the negated vertices of the variable gadget that corresponds to $x_i, i = 1, 2, \dots, n$, lie to the “left” side in $\Gamma(G_\phi)$, then variable x_i is set to true, otherwise x_i is set to false. We argue that this assignment satisfies ϕ . To realize this, observe that there exist three paths that emanate from each clause gadget. The one that emanates from the right endpoint of each clause gadget can never reach a false value. Therefore, each clause of ϕ must contain at least one true literal, and thus ϕ is satisfiable.

Conversely, suppose that there is a truth assignment that satisfies ϕ . We proceed to construct a RAC drawing $\Gamma(G_\phi)$ of G_ϕ , as follows: In the case where, in the truth assignment, variable $x_i, i = 1, 2, \dots, n$ is set to true, we place the negated vertices of the variable gadget that corresponds to x_i , to its left side in $\Gamma(G_\phi)$, otherwise to its right side. Since each clause of ϕ contains at least one true literal, we choose this as the right endpoint of its corresponding clause gadget. As mentioned above, it is always feasible to be connected to its variable gadgets by paths of length two. This completes our proof. \square

5 Conclusions

In this paper, we proved that it is \mathcal{NP} -hard to decide whether a graph admits a straight-line RAC drawing. Didimo et al. [7] proved that it is always feasible to construct a RAC drawing of a given graph with at most three bends per edge. If we permit one or two bends per edge, does the problem remain \mathcal{NP} -hard? The same question arises if the input graph has n vertices and exactly $4n - 10$ edges, i.e., whether the problem of recognizing the class of maximally dense RAC graphs is also \mathcal{NP} -hard.

⁴In Fig. 17, the corridors are the gray-shaded regions that reside at each variable gadget.

References

- [1] P. Angelini, L. Cittadini, G. Di Battista, W. Didimo, F. Frati, M. Kaufmann, and A. Symvonis. On the perspectives opened by right angle crossing drawings. In *Proc. of 17th International Symposium on Graph Drawing (GD09)*, volume 5849 of *LNCS*, pages 21–32, 2009.
- [2] E. N. Argyriou, M. A. Bekos, and A. Symvonis. Maximizing the total resolution of graphs. In *Proc. of 18th International Symposium on Graph Drawing (GD10)*, volume 6502 of *LNCS*, pages 62–67, 2010.
- [3] K. Arikushi, R. Fulek, B. Keszegh, F. Moric, and C. Toth. Graphs that admit right angle crossing drawings. In *Proc. of Graph Theoretic Concepts in Computer Science*, volume 6410 of *LNCS*, pages 135–146, 2010.
- [4] H. L. Bodlaender and G. Tel. A note on rectilinearity and angular resolution. *Journal of Graph Algorithms and Applications*, 8(1):89–94, 2004.
- [5] G. Di Battista, P. Eades, R. Tamassia, and I. G. Tollis. Algorithms for drawing graphs: an annotated bibliography. *Computational Geometry*, 4(5):235–282, 1994.
- [6] E. Di Giacomo, W. Didimo, G. Liotta, and H. Meijer. Area, curve complexity, and crossing resolution of non-planar graph drawings. In *Proc. of 17th International Symposium on Graph Drawing (GD09)*, volume 5849 of *LNCS*, pages 15–20, 2009.
- [7] W. Didimo, P. Eades, and G. Liotta. Drawing graphs with right angle crossings. In *Proc. of 12th International Symposium, Algorithms and Data Structures (WADS09)*, volume 5664 of *LNCS*, pages 206–217, 2009.
- [8] W. Didimo, P. Eades, and G. Liotta. A characterization of complete bipartite graphs. *Information Processing Letters*, 110(16):687–691, 2010.
- [9] V. Dujmović, J. Gudmundsson, P. Morin, and T. Wolle. Notes on large angle crossing graphs. In *Proc. of 16th Symposium on Computing: the Australasian Theory (CATS10)*, volume 109 of *Australian Computer Society*, pages 19–24, 2010.
- [10] P. Eades and G. Liotta. Right angle crossing graphs and 1-planarity. In *Proc. of 19th International Symposium on Graph Drawing (GD11)*, volume 7034 of *LNCS*, pages 148–153, 2011.
- [11] M. Formann, T. Hagerup, J. Haralambides, M. Kaufmann, F. Leighton, A. Symvonis, E. Welzl, and G. Woeginger. Drawing graphs in the plane with high resolution. *SIAM Journal of Computing*, 22(5):1035–1052, 1993.
- [12] M. Garey and D. Johnson. Crossing number is NP-complete. *SIAM Journal of Algebraic Discrete Methods*, 4(3):312–316, 1983.

- [13] M. R. Garey and D. S. Johnson. *Computers and Intractability: A Guide to the Theory of NP-Completeness*. W. H. Freeman, 1979.
- [14] A. Garg and R. Tamassia. Planar drawings and angular resolution: Algorithms and bounds (extended abstract). In *Proc. of 2nd Annual European Symposium on Algorithms (ESA94)*, volume 855 of *LNCS*, pages 12–23, 1994.
- [15] C. Gutwenger and P. Mutzel. Planar polyline drawings with good angular resolution. In *Proc. of 6th International Symposium on Graph Drawing (GD98)*, volume 1547 of *LNCS*, pages 167–182, 1998.
- [16] W. Huang, S.-H. Hong, and P. Eades. Using eye tracking to investigate graph layout effects. In *Proc. of 6th Asia-Pacific Symposium on Visualization 2007 (APVIS2007)*, IEEE, pages 97–100, 2007.
- [17] W. Huang, S.-H. Hong, and P. Eades. Effects of crossing angles. In *Proc. of IEEE VGTC Pacific Visualization Symposium 2008 (PacificVis 2008)*, IEEE, pages 41–46, 2008.
- [18] M. Kaufmann and D. Wagner, editors. *Drawing Graphs: Methods and Models*, volume 2025 of *LNCS*. Springer-Verlag, 2001.
- [19] C.-C. Lin and H.-C. Yen. A new force-directed graph drawing method based on edge-edge repulsion. In *Proc. of the 9th International Conference on Information Visualization*, pages 329–334. IEEE, 2005.
- [20] S. M. Malitz and A. Papakostas. On the angular resolution of planar graphs. In *Proc. of the 24th Annual ACM Symposium on Theory of Computing (STOC92)*, ACM, pages 527–538, 1992.
- [21] H. C. Purchase. Effective information visualisation: a study of graph drawing aesthetics and algorithms. *Interacting with Computers*, 13(2):147–162, 2000.
- [22] H. C. Purchase, D. A. Carrington, and J.-A. Allder. Empirical evaluation of aesthetics-based graph layout. *Empirical Software Engineering*, 7(3):233–255, 2002.
- [23] M. van Kreveld. The quality ratio of RAC drawings and planar drawings of planar graphs. In *Proc. of 18th International Symposium on Graph Drawing (GD10)*, volume 6502 of *LNCS*, pages 371–376, 2010.
- [24] C. Ware, H. Purchase, L. Colpoys, and M. McGill. Cognitive measurements of graph aesthetics. *Information Visualization*, 1(2):103–110, 2002.